GRANT
IN-26-CR
142850

p. 29

NASA Grant No. NAGW-2601

Microstructural Development During Directional Solidification of Peritectic Alloys

Final Technical Report

Grant Period: August 1, 1991 - September 30, 1992

Principal Investigator: Dr. Thomas A. Lograsso

Iowa State University
Ames, Iowa 50010

Microstructural Development During Directional Solidification of Peritectic Alloys

Introduction

Despite the widespread commercial use of peritectic alloys (e.g., steels, brass, bronze, intermetallic compounds, Co based superalloys and A_3B type superconductors), the characterization of the microstructural development during directional solidification of peritectics has historically lagged behind similar efforts directed towards other types of binary invariant reactions such as eutectic or monotectic. A wide variety of possible microstructures has been shown to form in peritectics [1-7] depending upon the imposed temperature gradient, G, the solidification velocity, V, as well as the presence or absence of convection in the melt. This has important technological implications since many commercially important alloys exhibit peritectics and processing methods such as casting and welding often involve widely changing conditions.

By the classical description of peritectic solidification the first phase to freeze, assumed here to be dendritic, reacts isothermally with the remaining liquid to form the secondary or peritectic phase. The reaction becomes diffusion limited after deposition of an initial layer of the peritectic product phase that envelops the parent primary solid. Often this results in the cessation of the peritectic reaction with the balance of the liquid solidifying in a non-equilibrium manner. At higher growth rates the peritectic reaction may be suppressed entirely resulting in the formation of the peritectic phase directly from the melt. At intermediate rates, the primary and peritectic phases grow side by side in a quasi- cooperative manner with the primary phase leading the peritectic phase by a distance l, which has been shown in previous work [4] to be a strong function of alloy composition, imposed temperature gradient and growth velocity.

A number of experimental studies of the directional solidification of peritectic alloys [1-3] have attempted to test the prediction of Chalmers [8,9] that conditions should exist where the phases α and β grow with a planer interface in a cooperative manner, similar to eutectic solidification, concluding for various reasons that cooperative growth is not possible.

Previous experimental studies at Iowa State University [4] have indicated that aligned, two phase growth of the α and β phases at a single isotherm is possible under very specific conditions of temperature gradient and growth velocity. The proper conditions are composition dependent and thus change continuously under terrestrial conditions as solidification progresses and rejected solute is convectively mixed into the remaining liquid. Results from previous work [4] shown in Figure 1, indicated that steady state growth does not occur and the separation distance between the phases decreases as the solid fraction is increased.

For solidification vertically upward of compositions less than the eutectic (56.3 % Bi) the lead-bismuth system is compositionally unstable to convection since the less dense component is rejected from the primary solid during solidification. Convection in the liquid has been recognized as an influencing factor in the microstructural development of peritectic alloys during solidification since it alters the compositional field in the liquid adjacent to the primary phase, inevitably affecting the morphology of the peritectic phase, but this effect has not been well documented. If strong convection

but this effect has not been well documented. If strong convection effects are present in the liquid, macrosegregation would result in significant composition changes as a function of fraction solidified. Since the interface characteristics are strongly composition dependent, the l spacing and even interface structure, would change with time. The only viable method of reducing the influence of convection on the microstructure, while maintaining other experimental parameters unchanged is by the utilization of a microgravity environment. Due to the infrequency and expense of flight experiments, parameters for such experiments must be carefully selected.

It has been the aim of this project to examine, in a systematic fashion, both experimentally and theoretically, the influence of gravitationally driven convection on segregation and microstructural development during solidification in peritectic systems under terrestrial conditions. The scientific results of the project will be used to establish ground based data in support of a meaningful microgravity flight experiment.

Theoretical Background

Existing models for peritectic solidification have focused exclusively on the morphology of the primary phase and have not addressed the morphology of the peritectic phase, assuming it forms via the peritectic reaction. Flemings and co-workers [11,12] were first to apply a simple constitutional supercooling criterion to the stability of multiphase planar liquid-solid interface in eutectic alloy systems. Brody and David [3] extended that application to describe the stability of a planar interface in a peritectic alloy system. With reference to the schematic peritectic phase diagram Figure 3a, this criterion states that, for S_1:

$$D_L(G/V) = m_1 C_o (1 - k_1) / k_1 \qquad (1)$$

For S_2:

$$D_L(G/V) = m_2 C_o(1 - k_2) / k_2 \qquad (2)$$

where D_L, G and V are the solute diffusion coefficient in liquid, the temperature gradient and the growth velocity, respectively. C_o is the bulk composition of the alloy, and m and k are the liquidus slopes and the equilibrium partition coefficients of the respective phases. These equations are plotted schematically as lines oa and obc in Figure 3b. The condition necessary for suppressing the primary (S_1) dendrite tips below the peritectic temperature, which is the equilibrium solidus for compositions between C_1 and C_2, has been presented by Bower et al. [13]. They show that an α to β transition is possible when:

$$\Delta T = D_L(G/V) > m_1 (C_L - C_o) \qquad (3)$$

where ΔT is the temperature differential between the liquidus and peritectic. This relationship is plotted as line abd in Figure 3b. The resulting figure is basically a morphological map showing the primary structure one might expect as a function of composition and growth conditions. It should be noted that this figure considers the

morphology of the primary or leading phase and does not consider the inevitable interaction with the trailing (peritectic) phase. In region A, at small values of G/V dendrites of the primary phase S_1 grow ahead of the peritectic isotherm and are surrounded by gradually thickening layer of the peritectic product (S_2) at temperatures below the peritectic isotherm. At higher values of G/V in region B, primary dendrites or cells of phase grow with higher tip undercoolings and S_2 will freeze at a planer front at the peritectic temperature. For higher bulk solute contents i.e.. region C, primary S_2 will grow with either a dendritic or cellular interface. For still higher values of G/V, region D and E, single phase S_1 or S_2 will grow with a planar front. Experimental results for Pb-Bi system have been found to give good agreement with the boundaries separating the morphological behavior of the alloys [3,4].

According to Brody and David's analysis [3], an α to β phase transition would occur at conditions represented by the line ab. Cooperative growth would therefore be anticipated for conditions at or just below line ab. There are two major drawbacks to their analysis. First, for a given composition, the α to β transition is predicted for a unique velocity. However, from our understanding of the dendrite to eutectic transition [13], one might expect the transition to occur at low as well as high velocities. Second, the transition line ab is calculated on the basis that β phase will form only if the interface temperature is below the peritectic temperature. This is indeed valid for the case considered by Brody and David in which the alloy was of peritectic composition. However, for hypoperitectic alloys it has been found by St. John and Hogan [14] that the solidification temperature of the β phase is higher than the peritectic temperature. Precisely what undercooling is required to form stable β phase cannot be predicted by the simple analysis used to obtain equation (3).

A better theoretical model was proposed by Jackson [15] for the dendrite to eutectic transition. If one can calculate the interface temperatures for the α and the β phases under given experimental conditions, then the phase with the higher interface temperature will be stable. Burden and Hunt [16] have used this criterion to show that the eutectic phase will be stable in two regimes, at very low and at very high velocities with a range of dendritic stability between. It would be interesting to examine if this criterion can be used to predict the transition in peritectic systems.

The interface temperatures of the α and β phases have been calculated using the theoretical model presented by Kurz et. al. [17]. Figure 4 shows the theoretical temperature profiles for the α and β phases as a function velocity for G = 17.8 K/mm in Pb-Bi alloys of compositions 30, 33 and 35 wt% Bi. The results show that the α phase is stable within a band of velocities between V_1 and V_2. Below V_1 and above V_2 the β phase is stable.

The low velocity transition is the same as that observed and modeled by Brody and David [3]. However, three important aspects must be realized. (1) The present model calculates the interface temperatures upon the assumption that the α or β phases are growing independently. In actuality, when α dendrites or cells form, the β phase is observed between the α dendrites or cells. Therefore, if the length of a cell or dendrite is small, the interaction between the α and β phases would be significant. This interaction would be greatest near the critical velocity, V_c. Furthermore, the interaction will be strongest when the interdendritic β phase is planar since the diffusion field ahead of the

planar β phase would be quite large at low velocities. This long range interaction may cause the transition velocity to differ significantly from the value calculated on the basis of Figure 3. (2) With interdendritic eutectics, the temperature of the eutectic front is fixed by the eutectic temperature since the undercooling at low velocities is negligible. However, in peritectic systems, interdendritic β phase can form over a range of temperatures. What determines the precise location of the β front is not yet well understood. Experimental studies are required to understand the criterion which establishes the interface temperature at which β dendrites or cells are formed. (3) The low velocity transition occurs at extremely low velocities where convection effects can become significant when the experiments are carried out in systems such as Pb-Bi in which density driven convection is present. Consequently, convection effects must be also be taken into account when predicting the transition velocity V.

Experimental Procedure

Material Preparation

Master alloys were prepared from 99.999 wt% lead and 99.91-99.999 wt% bismuth. Pre weighed amounts of the pure metals were melted, stirred under vacuum and then vacuum cast into 5 mm ID., 40 cm long Pyrex tubes utilizing an atmosphere of purified argon. The top and bottom of each sample blank were chemically analyzed by EDTA titration to determine the extent of macrosegregation. For a nominal composition of Pb-30 wt% Bi, the top and bottom compositions typically differed by less than .5 wt% Bi. Alloy sample blanks, 22 cm long x 5 mm OD, were then placed in 6 mm ID. quartz tubes for the unidirectional solidification experiments, resulting in a sample approximately 12 cm long x 6 mm OD. To reduce the sample diameter and utilize the existing experimental apparatus, 2.5 mm ID. plain carbon steel tubes were centered in the 5 mm Pyrex tubes and vacuum filled as before. Directional solidification of 22 cm sample blanks in the 6 mm ID. tubes resulted in samples approximately 9 cm long x 2.5 mm OD.

Experimental Apparatus

The unidirectional solidification apparatus used in this study has been described in detail by Mason [18]. The main parts of this apparatus are shown in Figure 5. The sample tube remains stationary and the temperature gradient is setup by the temperature difference between the furnace and a cooling chamber. The furnace and cooling chamber are moved upward by the drive mechanism at the desired velocity until the required fraction of steady state growth has occurred, at which time the sample is quenched, sectioned and examined metallographically.

Temperature Gradient Control

During the unidirectional solidification experiments, the temperature gradient in the sample was controlled by the temperature of the furnace since the cooling chamber temperature remained relatively constant. The furnace was maintained at 650 C, yielding an average temperature gradient in the liquid ahead of the solidification front of 17.8

K/mm. The presence of the steel tube in the 2.5 mm samples tended to reduce the gradient by approximately 18%.

Growth Rate Control.

The solidification velocity was controlled by the drive mechanism which moved the furnace and cooling chamber upward at a predetermined rate as shown in Figure 5. The velocity of the thermal assembly depends on the speed of the stepping motor, which was controlled by a Commodore PET 2001 computer interfaced to the Compumotor driver. The velocity was calibrated by using a linear variable differential transformer and could be verified by correlation with the solidification distance over the solidification time. Samples were solidified at velocities of .75 and 2 μm/s.

Temperature Measurements

Thermal profiles were obtained during solidification by placing a K type thermocouple at the desired position along the ingot axis and acquiring data at 2 min. intervals utilizing a Macintosh classic II interfaced to a Keithly digital microvolt meter. Data was obtained until both the primary and peritectic phase fronts passed the thermocouple bead. The evolution of latent heat due to the freezing of the primary phase left a discernible slope change permitting accurate determination of the α front temperature by numerically differentiating the thermal profile data. Temperature gradients could be obtained from the slope just ahead of the front. Unfortunately the latent heat from the β phase was insufficient to discern the β front temperature except when β was the only phase to form and it was subsequently estimated from the temperature profiles and the measured lag distance behind the primary front.

Microstructural Observations.

The first 3 cm of the samples were solidified at a high rate (500 μm/s) to avoid initial thermal transients and ensure a steady state thermal profile. The sample was then stopped and allowed to equilibrate. Unidirectional solidification was then carried out at the chosen rate until the desired fraction of the sample was solidified at which time the sample was quenched to preserve the interface structure. A longitudinal section containing the interface was prepared to determine the distance l, between the primary and peritectic phase fronts. Samples were conventionally polished through 600 grit SiC and then electropolished. Phase contrast was sufficient in the as electropolished condition for optical metallography.

Results

Experiments were carried out in which the fraction solidified was varied from about 0.2 to over 0.9 for solidification velocities of .75 and 2 μm/s. At 2 μm/s the structure consisted of primary α dendrites followed by dendritic β. Figure 6 shows the effect of fraction solidified on the interface morphology for a Pb-30 wt% Bi alloy solidified with G= 17.8 K/mm and V=2 μm/s. In Figure 6a , at a solid fraction of .38, primary α leads β by a distance of 1.35 mm. At a fraction solid of .55 (Figure 6b) the distance has decreased to .94 mm. By the time the solid fraction has reached .78 (Figure

6c) the distance has decreased to .45 mm and the volume fraction of α has noticeably decreased. At a solid fraction of .95 (Figure 6c) the composition has increased to the point where the α phase is no longer present and the structure consists of primary β dendrites with interdendritic eutectic.

Figure 7 shows the effect of fraction solidified on the interface structure for samples solidified at .75 μm/s. In Figure 7a at a solid fraction of .29, cellular α leads the planer β phase by a distance l= 1.4 mm. At a solid fraction of .53 (Figure 7b), l has decreased to .25 mm and the volume fraction of α has also decreased indicating an increase in Bi concentration. At a solid fraction of .73, Figure 7c, the composition has increased to the point that the critical conditions have been exceeded and single phase, planer β is observed. Finally in Figure 7d at a solid fraction of .91, conditions are such that the planer β becomes unstable and cellular β with interdendritic eutectic results.

Figures 8 and 9 show the measured l spacing as a function of fraction solid for a Pb 30 wt% Bi alloy, G= 17.8 K/mm, at velocities of .75 and 2 μm/s respectively. Data is shown for both 6 mm and 2.5 mm diameter samples. A systematic decrease in phase separation was observed for both velocities as the fraction solidified was increased. The rate of decrease was greater at the slower speed where the a structure was cellular indicating greater convection and macrosegregation then at the higher speed where the α structure was dendritic.

In an attempt to reduce convection and macrosegregation, the sample diameter was reduced from 6 mm to 2.5 mm. This resulted in a shift upward for both velocities attributable primarily to the decrease in temperature gradient resulting from the presence of the 22 cm steel sample tube, however, the rate of change of composition as evidenced by the slope was unchanged for a given velocity.

When the l spacings are normalized by the temperature gradient, the data can be represented by single line at low fractions solid as shown in Figures 10 and 11 for the 2 and .75 μm/s samples respectively, indicating that the measured spacing scales linearly with the imposed temperature gradient. At higher solid fractions (greater than .8), large compositional changes result in a relatively rapid decrease in l. Data is also shown in Figure 10 for samples from previous work [4].

Results of the measured α and β interface temperatures as a function of fraction solidified are shown in Figures 12 and 13. At V=2 μm/s (Figure 12), the β interface temperature was above the peritectic temperature for all fractions solid. This is consistent with St. John and Hogan's [14] observations of β front temperature in the same system.The microstructural observations are in good agreement with those of Brody and David [3] for the Pb-Bi system. The basic theoretical ideas, presented in Figure 3 appear to be valid in that with increasing G/V, the α phase dendrites become cells which decrease in length until the critical conditions have been reached at which point both and phases grow cooperatively. Above this critical condition , only the peritectic phase is found.

Discussion

The compositional increase which occurs as a function of fraction solidified was verified in previous work [4] for conditions where the microstructure consists of dendritic α followed at relatively large distances by non planer β. Under these

conditions, lateral distribution of solute and the relatively low permeability of the dendritic array inhibit convective interchange of liquid with the mushy zone and result in a smaller compositional increase than might be predicted. A more severe increase approaching that given by the Scheil Equation would be expected at lower velocities, where the structure is cellular α and planer β with a relatively short distance between phases enhancing convective flow resulting in more complete liquid mixing.

As solidification progresses and rejected Bi is convectively mixed into the liquid the l spacing decreases approaching and eventually surpassing the critical (G,V,C) condition for cooperative or coupled growth. The phases are not coupled in the lamellar eutectic sense but rather analogs to a divorced or faceted/nonfaceted eutectic where one phase often leads the other and the close proximity of the phases necessitates overlapping diffusion fields. It is therefore not possible in a terrestrial environment, to maintain the conditions necessary for combined growth of both phases at a common planer front other than as a brief transient.

Results of calculations for tip temperatures shown in Figure 4 can be used to estimate a theoretical separation distance as a function of velocity and composition by multiplying the ΔT between the phases by the measured temperature gradient. This approach assumes no interaction between the phases and diffusional mixing only (no convection) in the melt. Figure 14 shows the theoretical separation distance as a function of velocity for the 6 mm diameter samples of 30 wt% Bi. Repeating the calculations for compositions ranging from 30-36 wt% Bi permits determination of the theoretical length as a function of composition. Figure 15 shows the theoretical l as a function of composition for a velocity of 2 μm/s.

If one now assumes that the liquid is completely mixed, the liquid composition at the primary interface as a function of fraction solid can be represented by the Scheil equation as shown in Figure 16 for a 30 wt% Bi alloy. Assuming that the liquid is completely mixed by convection, one might expect to observe primary α up to a solid fraction of approximately .42 followed by primary β to a solid fraction of .95 with the balance solidifying as a two phase eutectic mixture. Experimentally we observe primary α up to a solid fraction of .59 in the .75 μm/s samples and approximately .8 in the 2 μm/s samples. This indicates that convection and the resulting segregation is more severe at the lower rate.

Combining the results from Figures 15 and 16, it is possible to come up with a theoretical length as a function of fraction solid as shown in Figure 17. The measured results for the 2 μm/s samples (both 2.5 and 6 mm diameter) are also shown in Figure 17. It can be seen that the theoretical results under predict the length in all cases. This should not be surprising since the assumption was made that the phases are growing independently. In actuality, the presence of the leading α phase and its lateral rejection of solute causes the liquid ahead of the β phase to be enriched in Bi faster than if the β phases were indeed growing independently. Since the β is growing from a liquid of higher composition, it will grow at a lower temperature resulting in an increased lag distance for a given temperature gradient.

If one assumes that the α and β phase fronts are in local equilibrium, then it is possible to estimate the interface composition as a function of solid fraction utilizing the measured interface temperature profiles (Figures 12 and 13) and the equilibrium phase

diagram (Figure 2). Figure 18 shows the estimated interface composition as a function of solid fraction for the 6 mm diameter samples solidified at a velocity of .75 is μm/s. The results from Scheil calculations are also shown for comparative purposes. Since the Scheil equation assumes complete liquid mixing it can be thought of as an upper bound to the degree of segregation in the alloy. The liquidus curve on the equilibrium phase diagram can be considered to be a lower bound. It can be seen that the experimental results follow Scheil quite closely, indicating the liquid is completely mixed by convection.

The results for the 2 μm/s samples are shown in Figure 19. They do not follow Scheil very closely as may be anticipated since at that velocity both phases are dendritic (the Scheil equation is strictly derived for plane front growth). The complex and tortuous structure of the two phase dendritic structure would serve to limit convective interchange of liquid with the mushy zone and lead to a lower degree of macrosegregation than in the .75 μm/s samples.

Conclusions

(1) The separation distance, l, between the α and b fronts is found to decrease as the fraction solid is increased for constant V and G conditions.

(2) Convection effects at low velocity resulted in extensive macrosegregation which manifests itself in severe microstructural changes as a function of fraction solidified, particularly at lower velocities.

(3) Convection and macrosegregation during solidification prevent the establishment of the conditions necessary for steady state two phase growth at a common isotherm.

(4) Reduction of sample diameter from 6 mm to 2.5 mm had no effect on the extent of convection and macrosegregation.

(5) Measured beta interface temperatures are observed to be above the peritectic isotherm for all fractions solid in the 2 μm/s samples.

(6) Calculation of theoretical phase separation distance (l) assuming no interaction of the phases under predicts the observed l spacings in all cases.

(7) The composition profile as a function of fraction solid determined by assuming local equilibrium is closely approximated by the Scheil equation at .75 μm /s but are significantly lower at 2 μm/s where both phases are dendritic.

(8) Utilization of a microgravity environment remains the only viable method of reducing convection and macrosegregation while maintaining other experimental parameters unchanged and should permit maintenance of the critical conditions necessary for cooperative two phase growth at a common isotherm.

References

1. D. R.Uhlmann. and G. A. Chadwick, Acta. Met., Vol. 9, (1961), pp. 835-840.

2. W. J. Boettenger, Met. Trans. Vol. 5, (1974), pp. 2023-2031.

3. H. D. Brody and S. A. David, Int. Conf. Solidification and Casting, Sheffield, July 1977, pp. 144-151.

4. B. C. Fuh, PhD Dissertation, Iowa State University, 1984

5. N. J. W. Barker and A. Hellawell, Mat. Sci., Vol. 8, (1974), pp. 353-356.

6. A. P. Titchener and J. A. Spittle, Acta. Met., Vol. 23, (1975), pp. 497-502.

7. A. Ostrowski and E. W. Langer, Int. Conf. Solidification and Casting, Sheffield, July 1977, pp.139-143.

8. B. Chalmers, Physical Metallurgy, John Wiley and Sons, New York, 1959, pp. 271-272.

9. B. Chalmers, Principles of Solidification, John Wiley and Sons, New York,1963, pp. 224-227.

10. B. Predel and W. Schwerman, Z. Metallkde, Vol. 58, (1967), pp. 553-557.

11. F. R. Mollard and M. C. Flemings, Trans. TMS-AIME, Vol. 239, (1967) pp. 1526-1546.

12. M. D. Rinaldi, R. M. Sharp, and M. C. Flemings, Met. Trans., (1972), Vol. 3, pp. 3133-3148.

13 T. F. Bower, H. D. Brody and M. C. Flemings, Trans. Metall. Soc. AIME, Vol. 236, (1966), pp. 624

14. D. H. St. John and L. M. Hogan, J. of Mat. Sci., Vol. 17, (1982), pp. 2413-2418.

15. K. A. Jackson, Trans. Metall. Soc. AIME, Vol. 242, (1968), pp. 1275.

16. M. H. Burden and J. D. Hunt, J. Cryst. Growth, 22 (1974) 109.

17. W. Kurz, B. Giovanola and R. Trivedi, Acta Met., 14, Vol. 5 (1986), pp.823-830

18. J. T. Mason: An Apparatus for Directional Solidification, IS- 4817,UC-37, Nov.1982
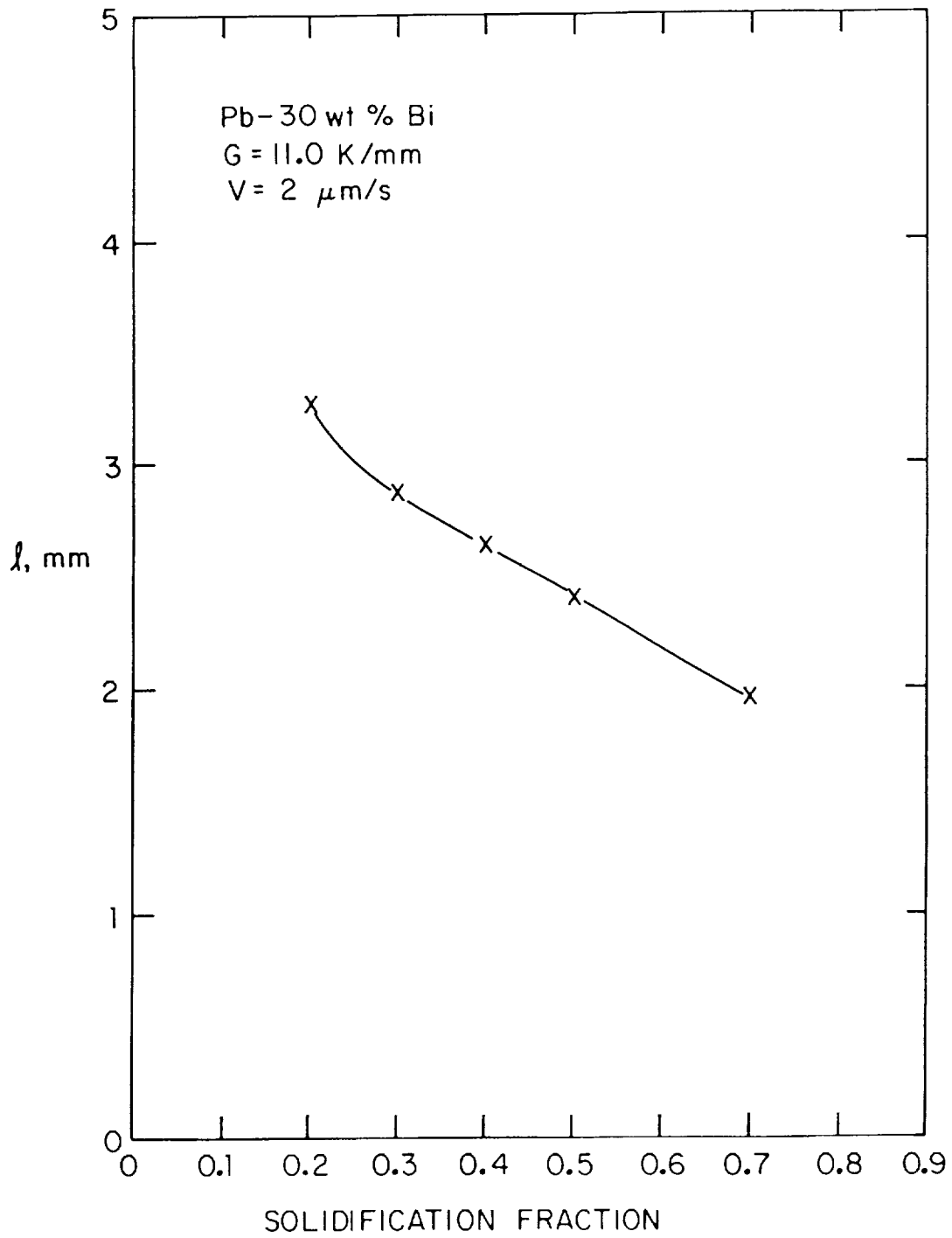
Figure 1. L as a function of fraction solid for Pb-30wt.% Bi , G=11 K/mm, V=2 μm/sec.[4]
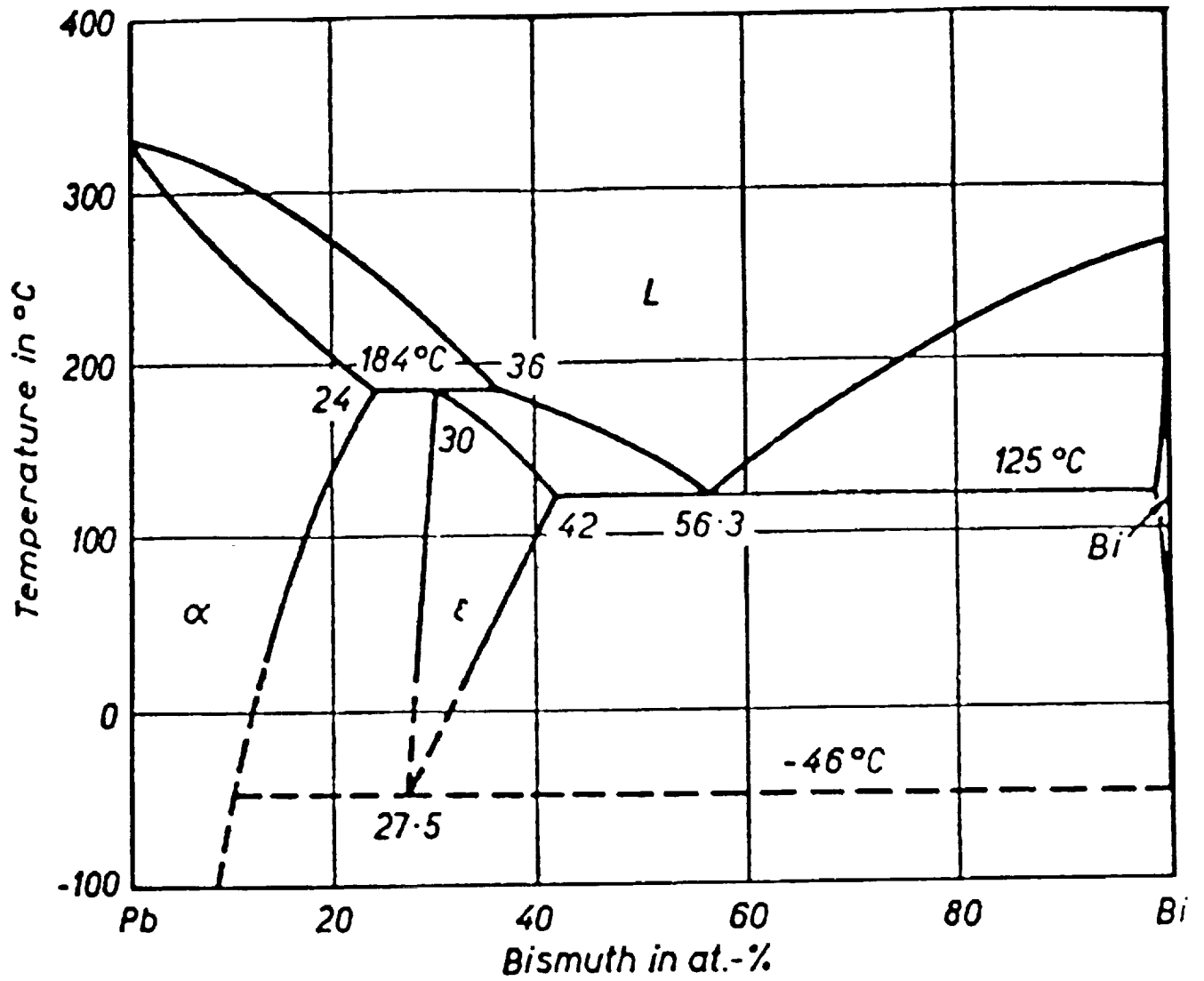
Figure 2. The Pb-Bi equilibrium phase diagram. [10]
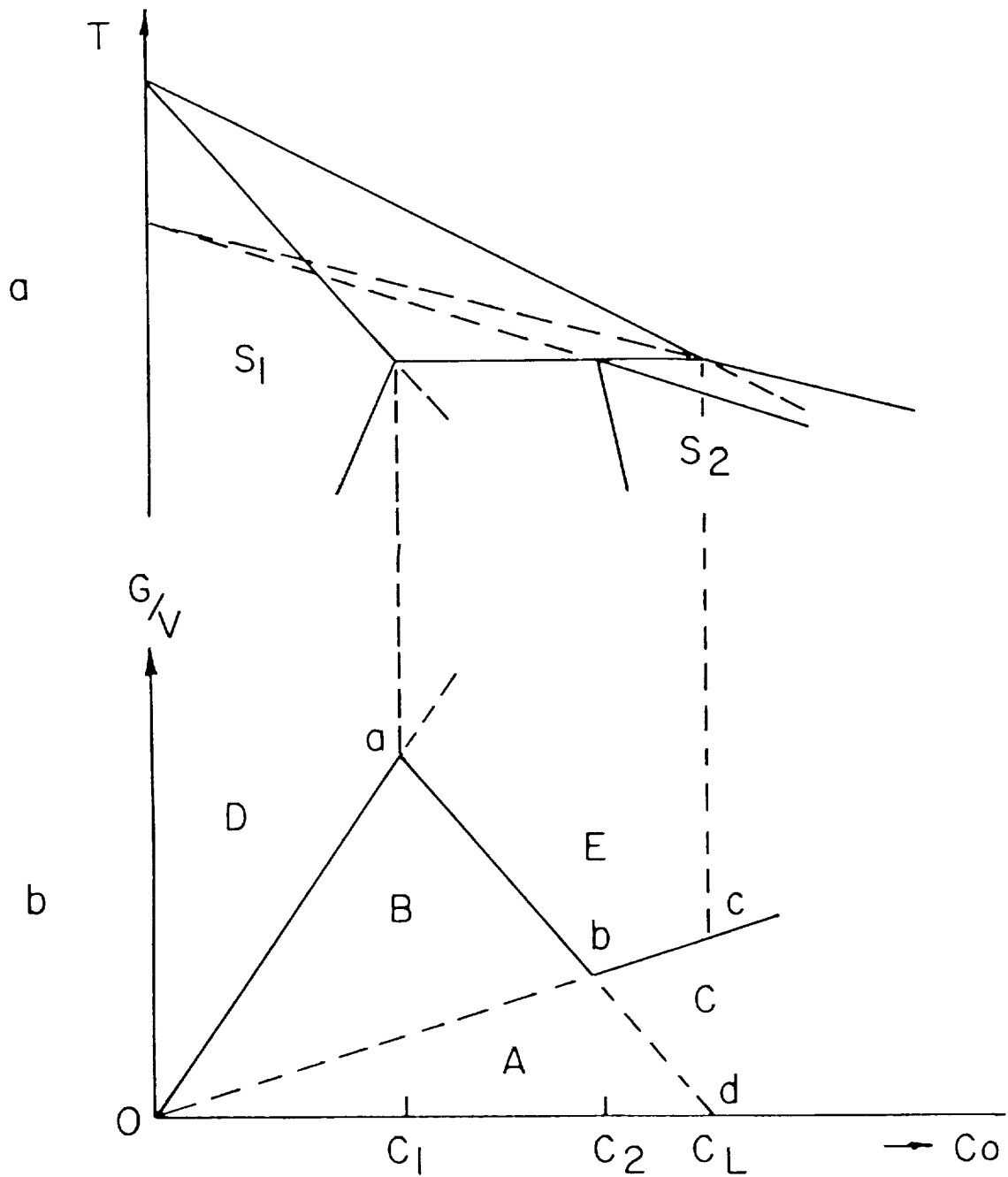
Figure 3. A schematic phase diagram for a peritectic system and critical G/V vs. C_0 plot to obtain a planar solid/liquid interface. Expected microstructures and interface morphology are also shown as: A-primary dendrites of S1 surrounded by S2, B-rods of S1 followed by planar S2; C-cellular or dendritic S2; D- single phase planar S1; and E-single phase planar S2. From reference [3].
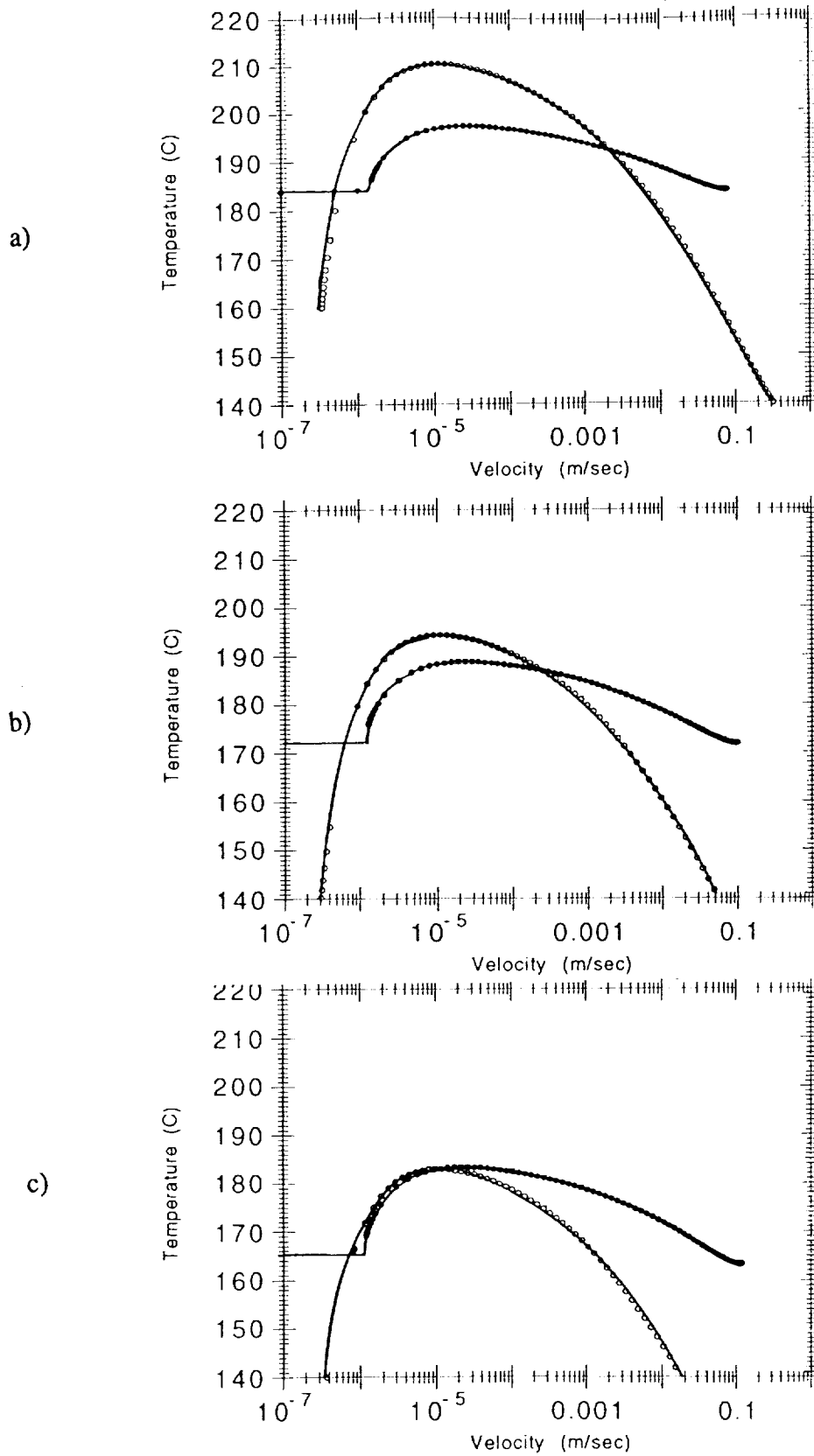
Figure 4. The theoretical tip temperature versus growth rates at G=17.8K/mm for alloy compositions of a) 30, b) 33, and C) 35. wt.% Bi.
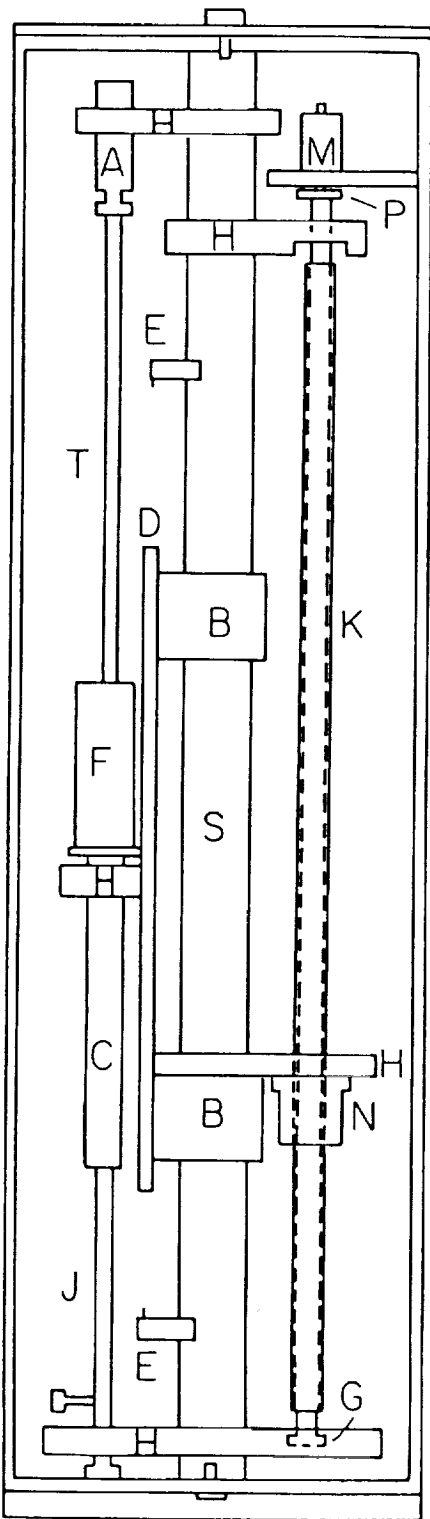
A   Top sample assembly
B   Square support base
C   Cooling Chamber
D   Drive plate
E   Limiting switch
F   Furnace
G   Ball bearing support
H   Clamp
J   Bottom support base
K   Ball bearing screws
M   Stepping motor
N   Ball bearing nut & flange
P   Timer belt pulley
S   Square shaft
T   Sample tube

Figure 5. The main elements of directional solidification apparatus.
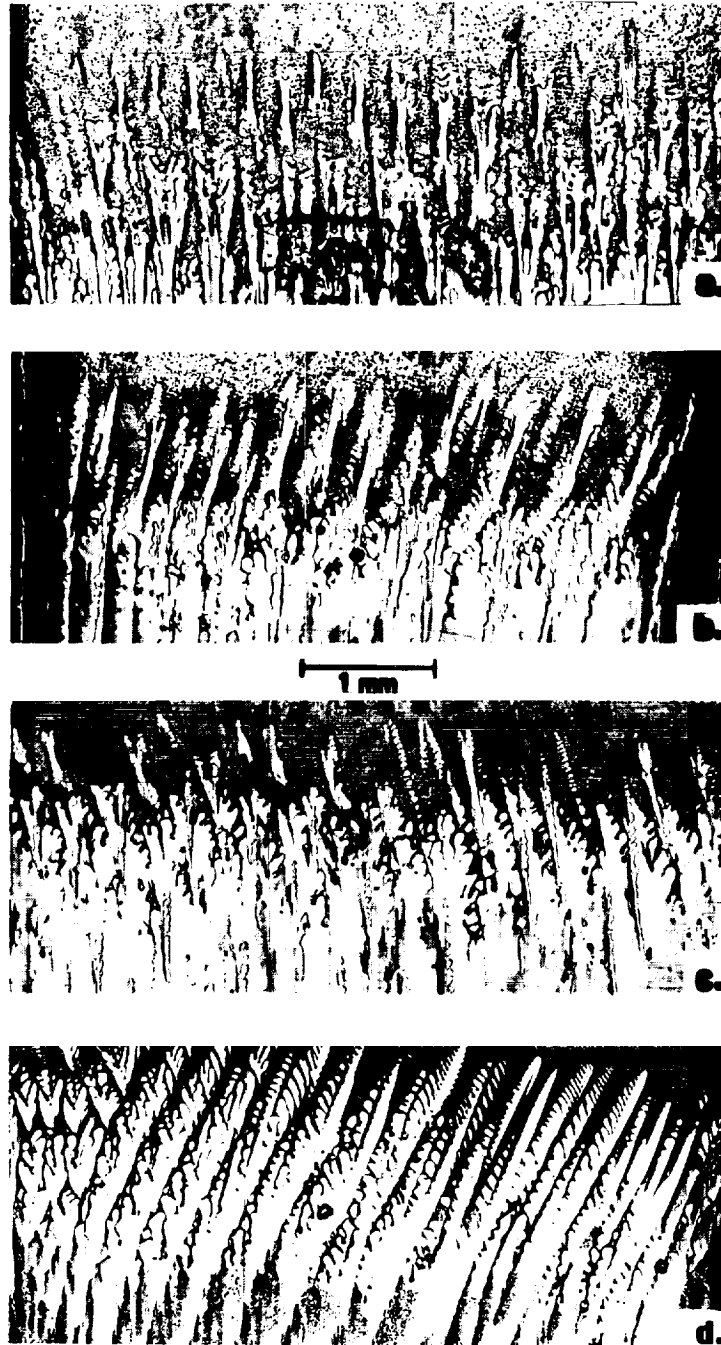
Figure 6. Interface structure as a function of fraction solid for Pb-30 wt.% Bi alloys at G = 17.8 K/mm and V = 2μm/sec. f_S = a) .38 b) .55 c) .78 d) .95.
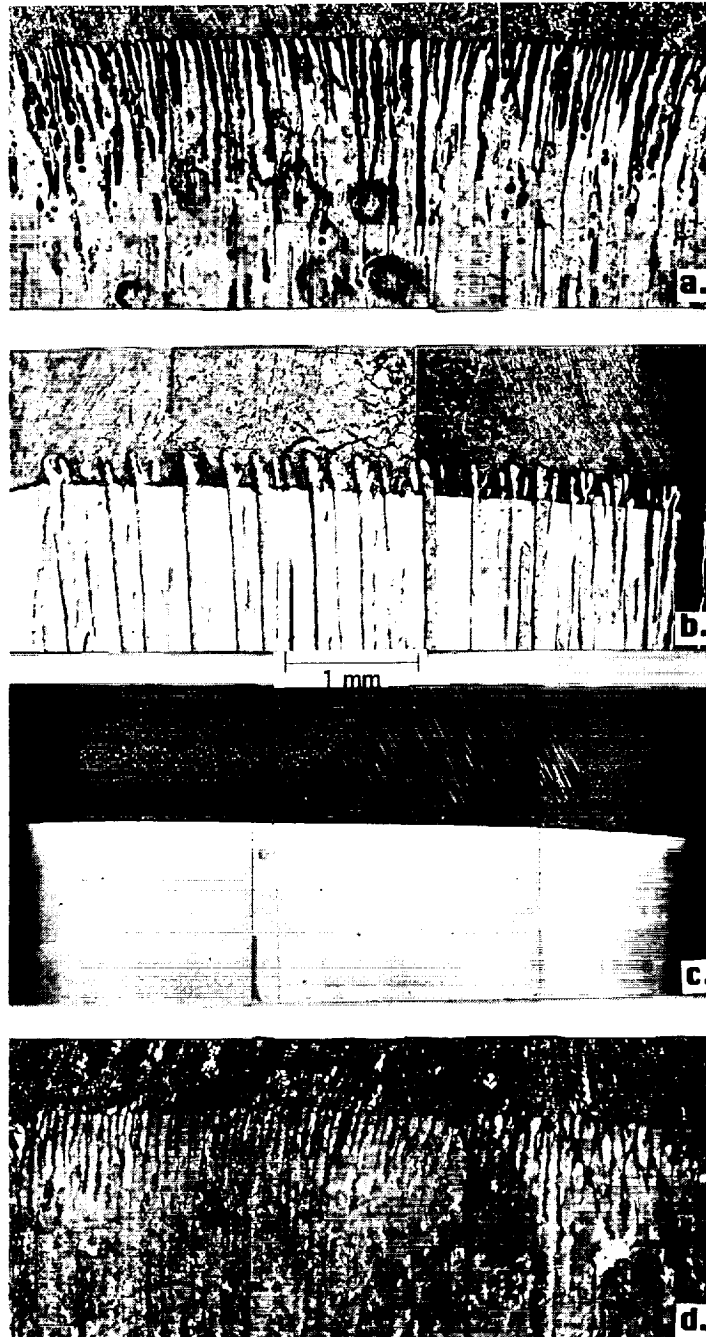
Figure 7. Interface structure as a function of fraction solid for Pb-30wt.% Bi alloys at G = 17.8 K/mm and V =.75 μm/sec. f_S = a) .29 b) .53 c) .73. d).91
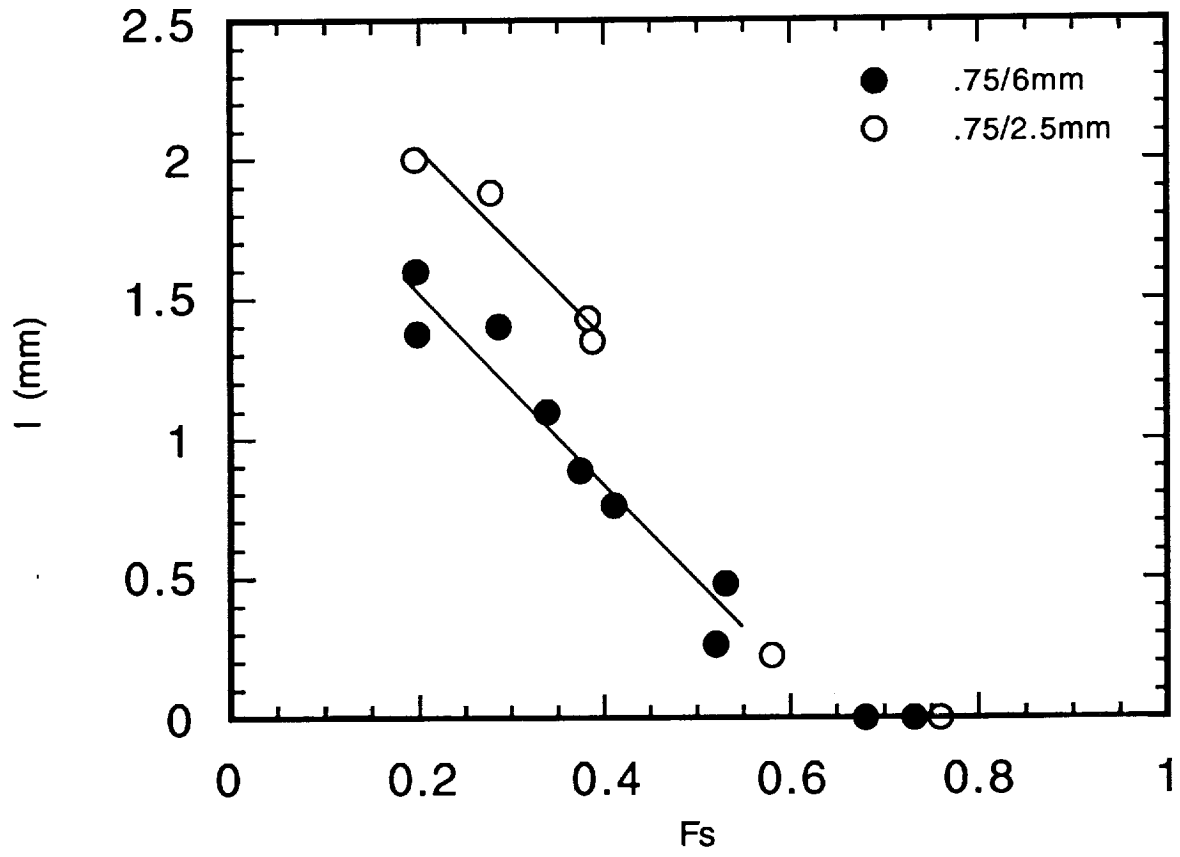
Figure 8. l vs fraction solid for Pb-30 wt.% Bi alloys.solidified at V=.75 μm/sec.
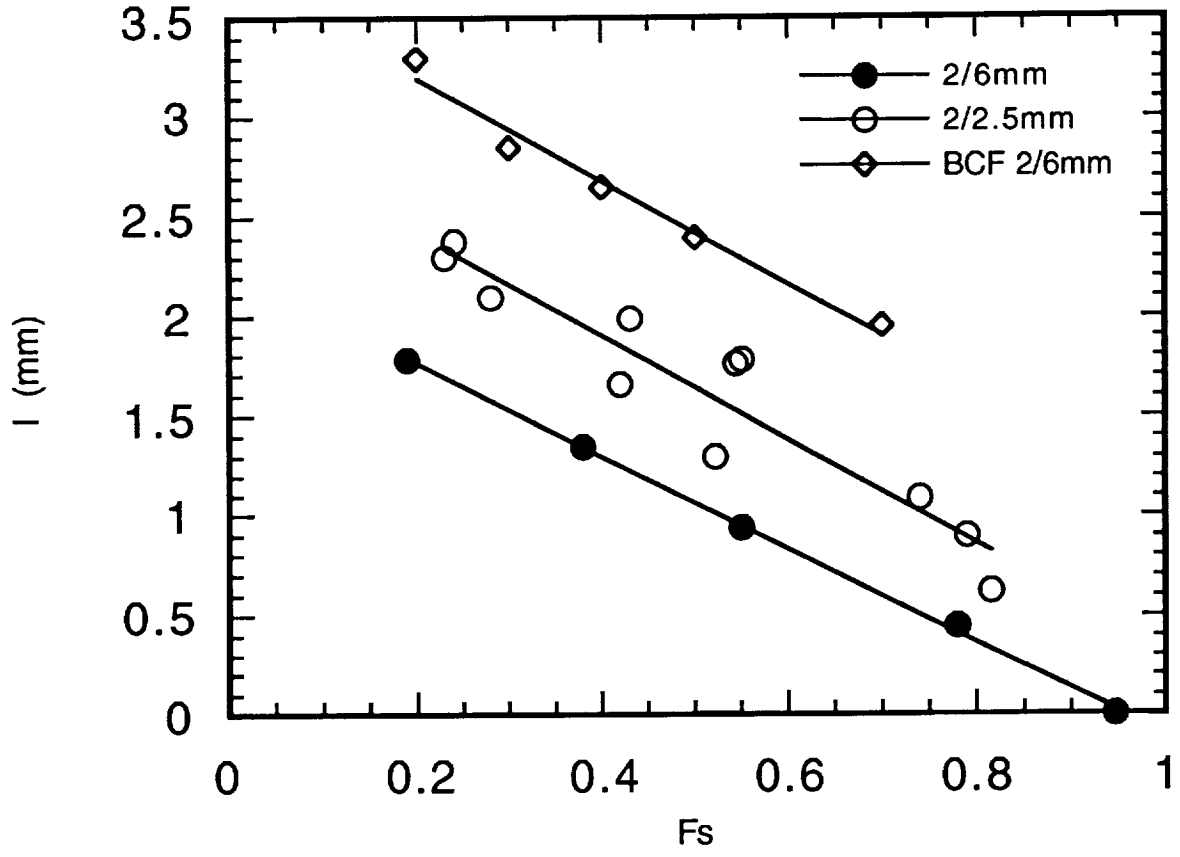
Figure 9. l vs fraction solid for Pb-30 wt.% Bi alloys solidified at V=2 μm/sec.
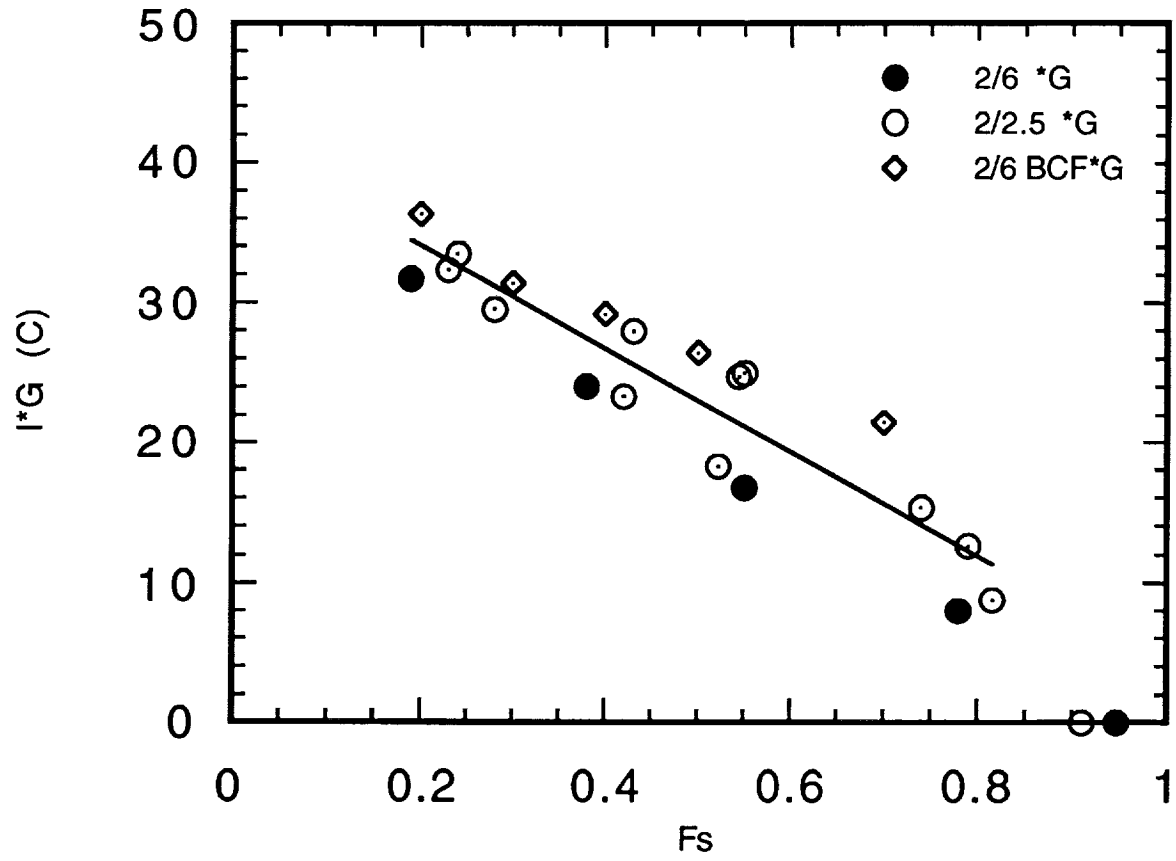
Figure 10. l vs fraction solid normalized by the temperature gradient for Pb-30 wt.% Bi alloys.solidified at V=2 μm/sec.
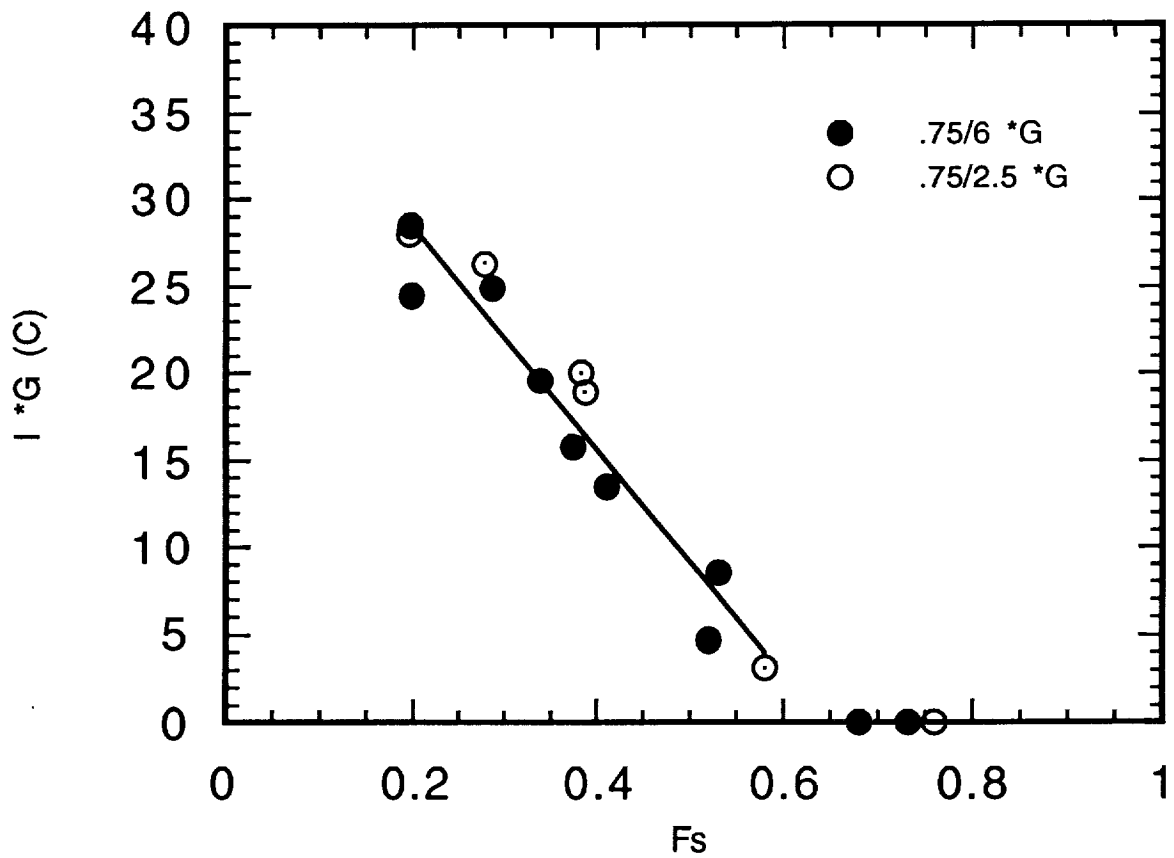
Figure 11. 1 vs fraction solid normalized by the temperature gradient for Pb-30 wt.% Bi alloys solidified at V=.75 µm/sec.
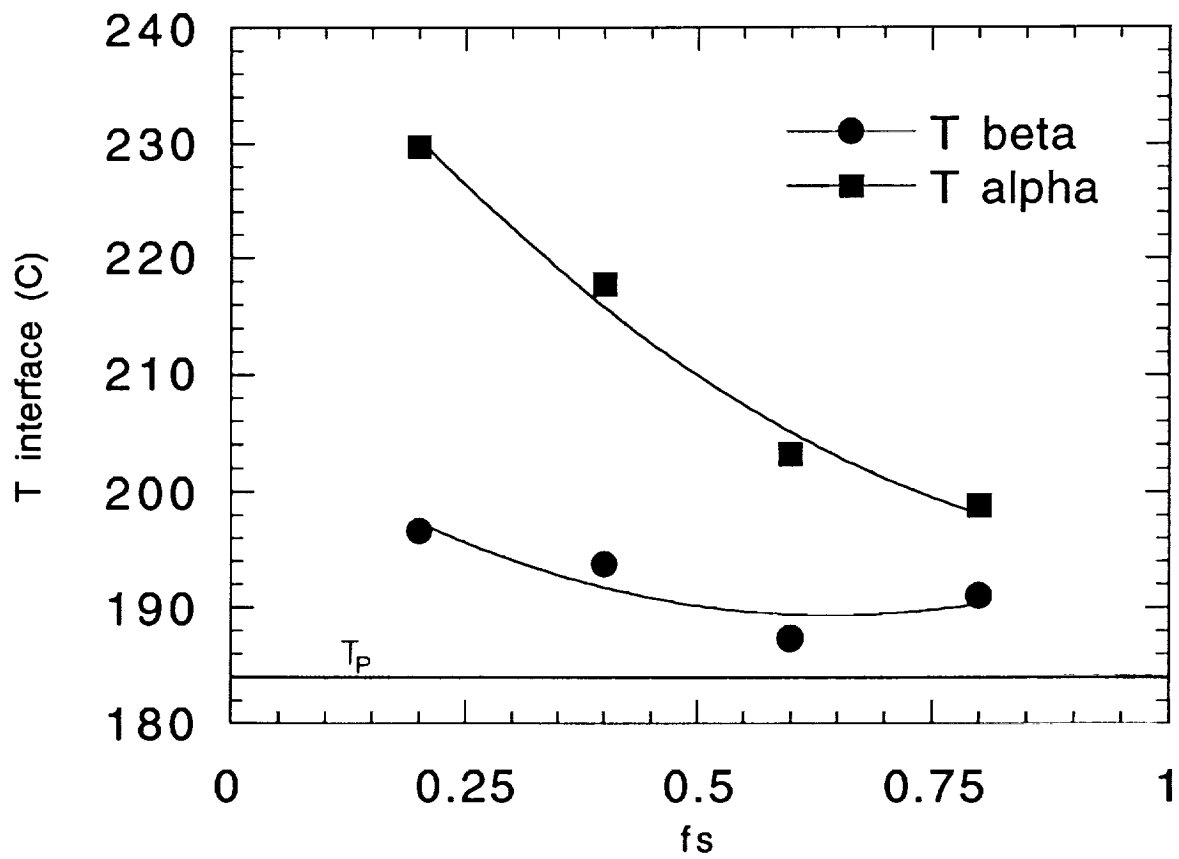
Figure 12. Measured alpha and beta interface temperatures as a function of fraction solid for samples solidified at V=2 μm/sec.
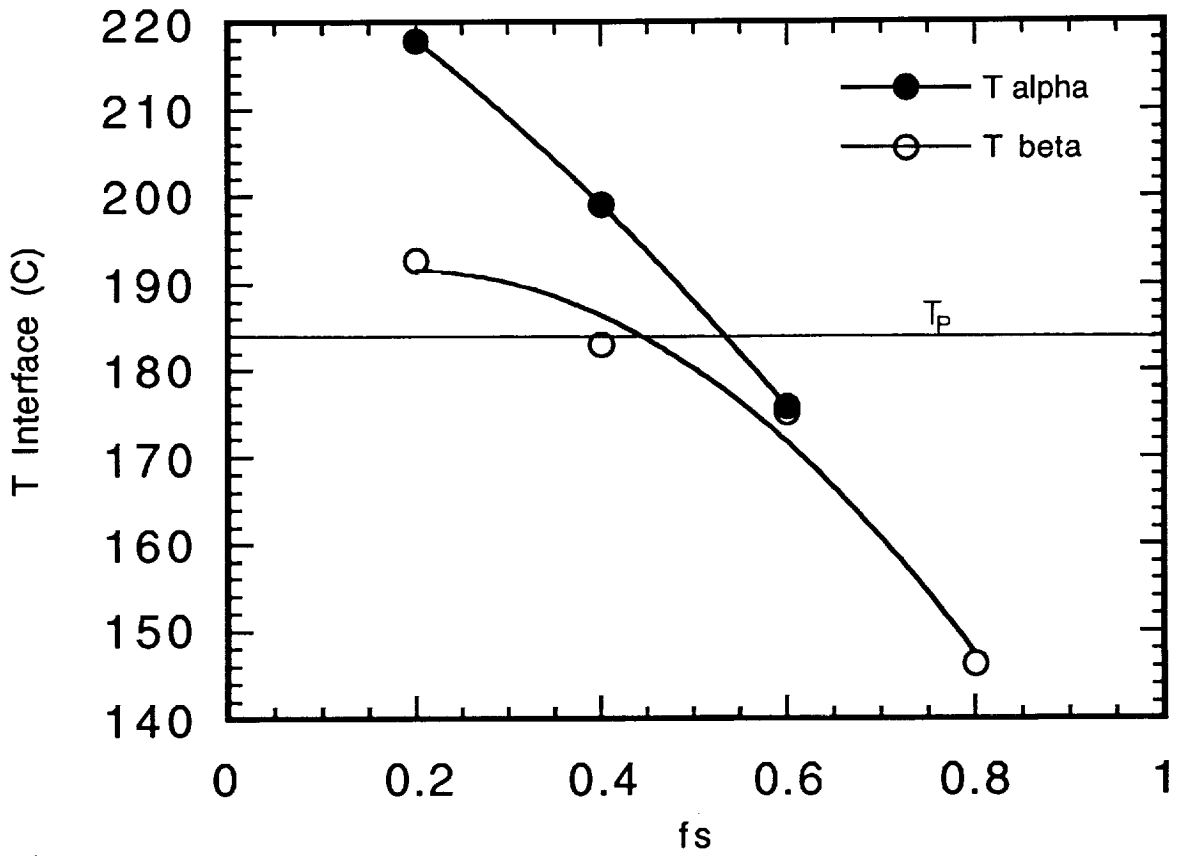
Figure 13. Measured alpha and beta interface temperatures as a function of fraction solid for samples solidified at V=2 μm/sec.
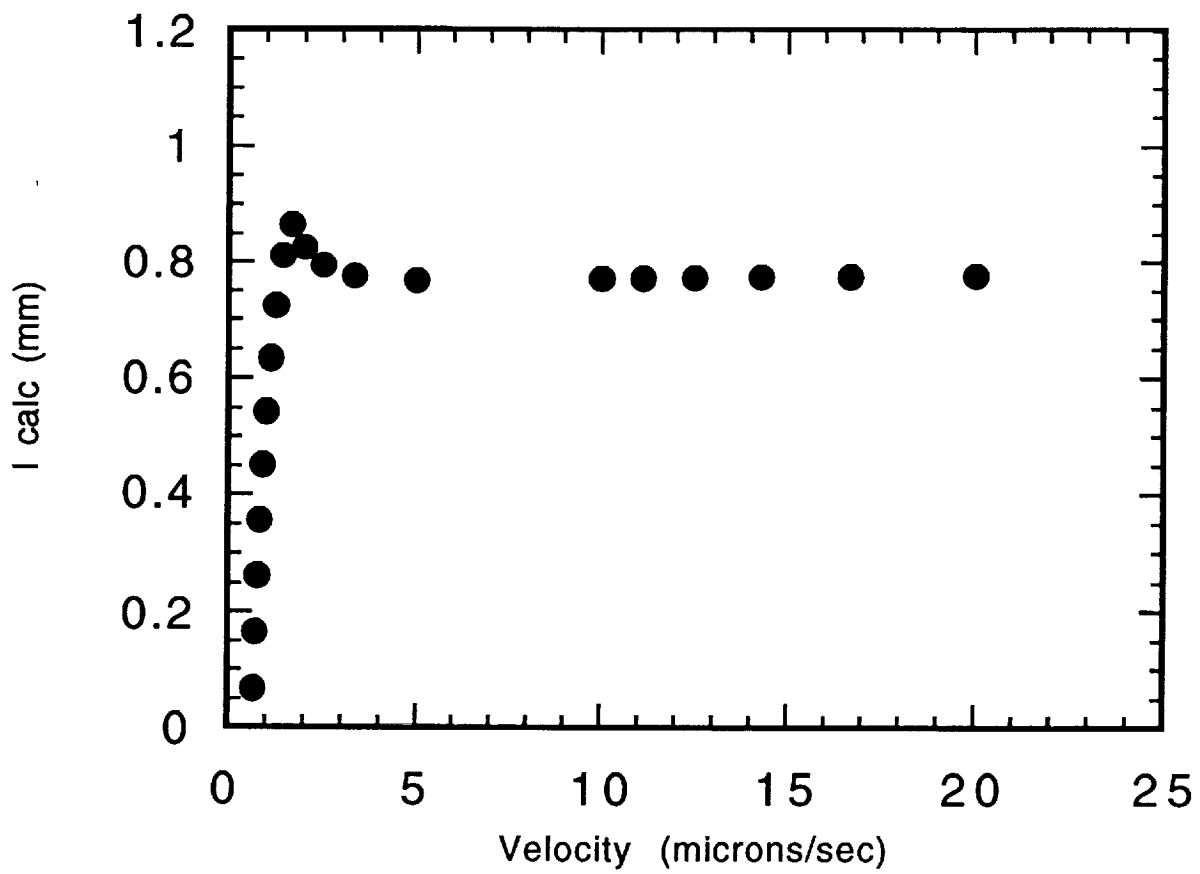
Figure 14. Calculated lag distance l, as a function of velocity for 30 wt.% Bi alloys.
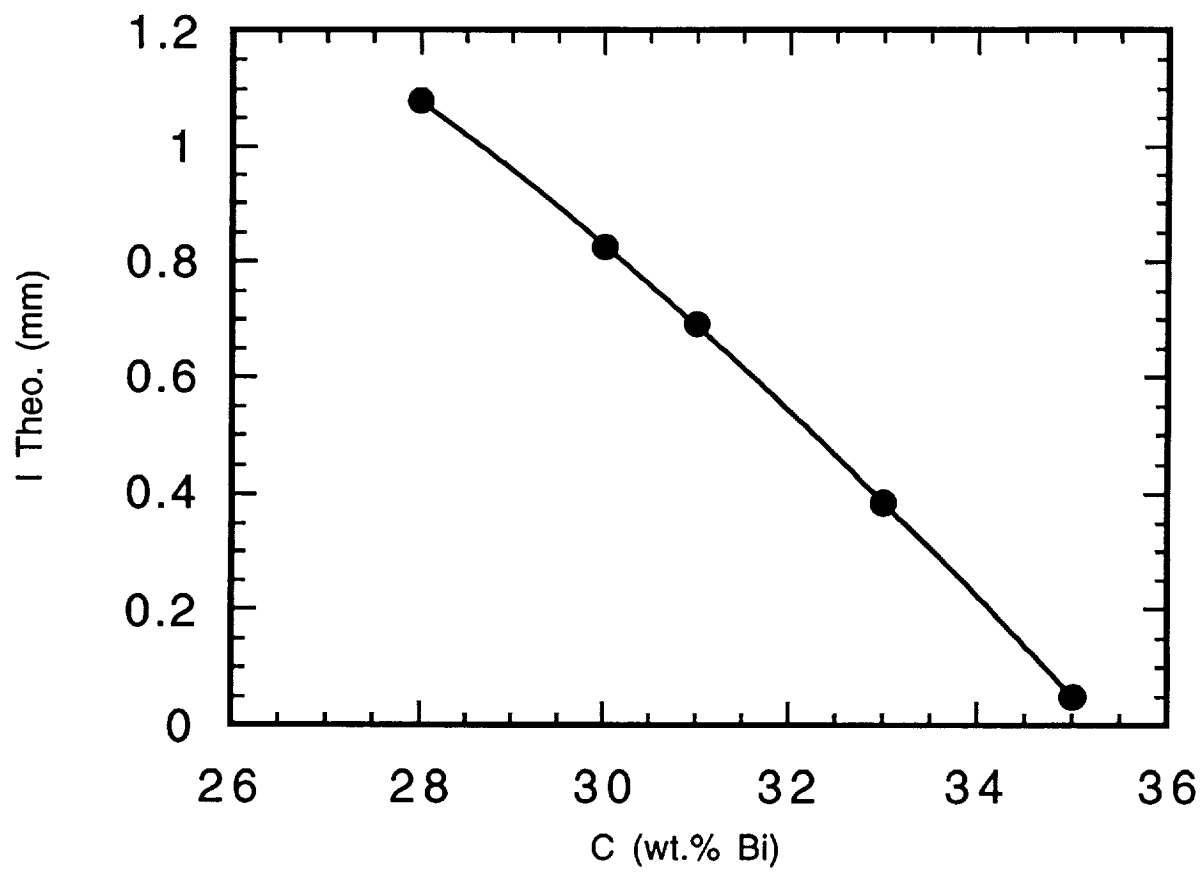
Figure 15. Theoretical lag distance as a function of composition for V=2 μm/sec.
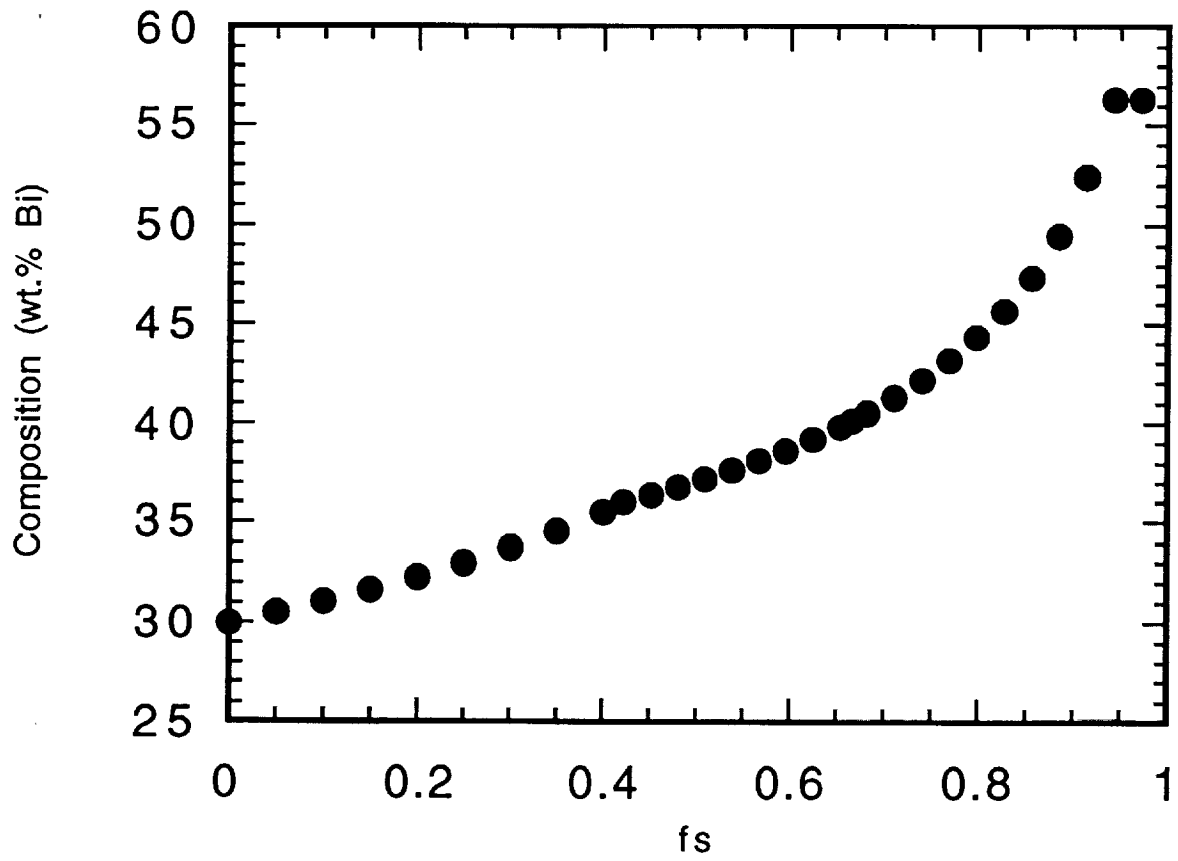
Figure 16. Theoretical composition as a function of fraction solid for a 30 wt.% Bi alloy as determined By the Scheil equation.
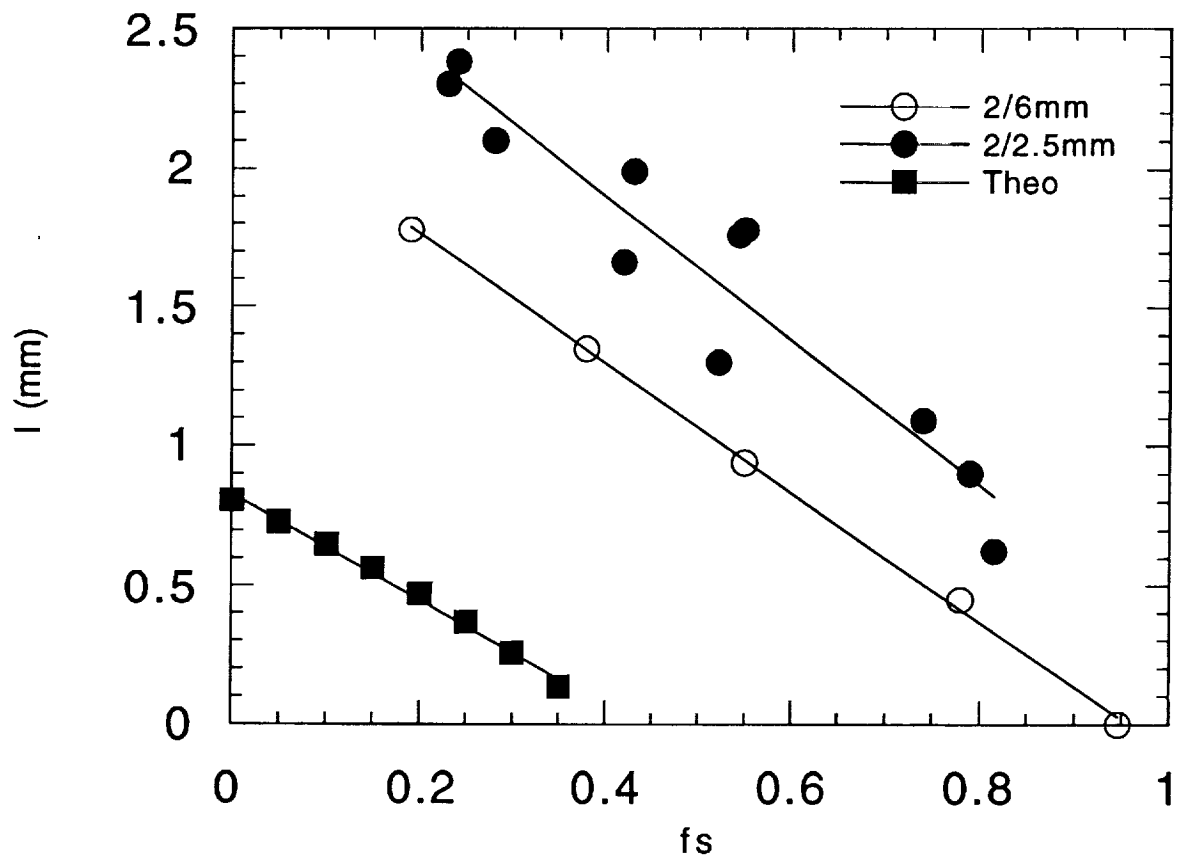
Figure 17. Comparison of measured and calculated l as a function of fraction solid for 30 wt.% Bi samples solidified at V=2 μm/sec.
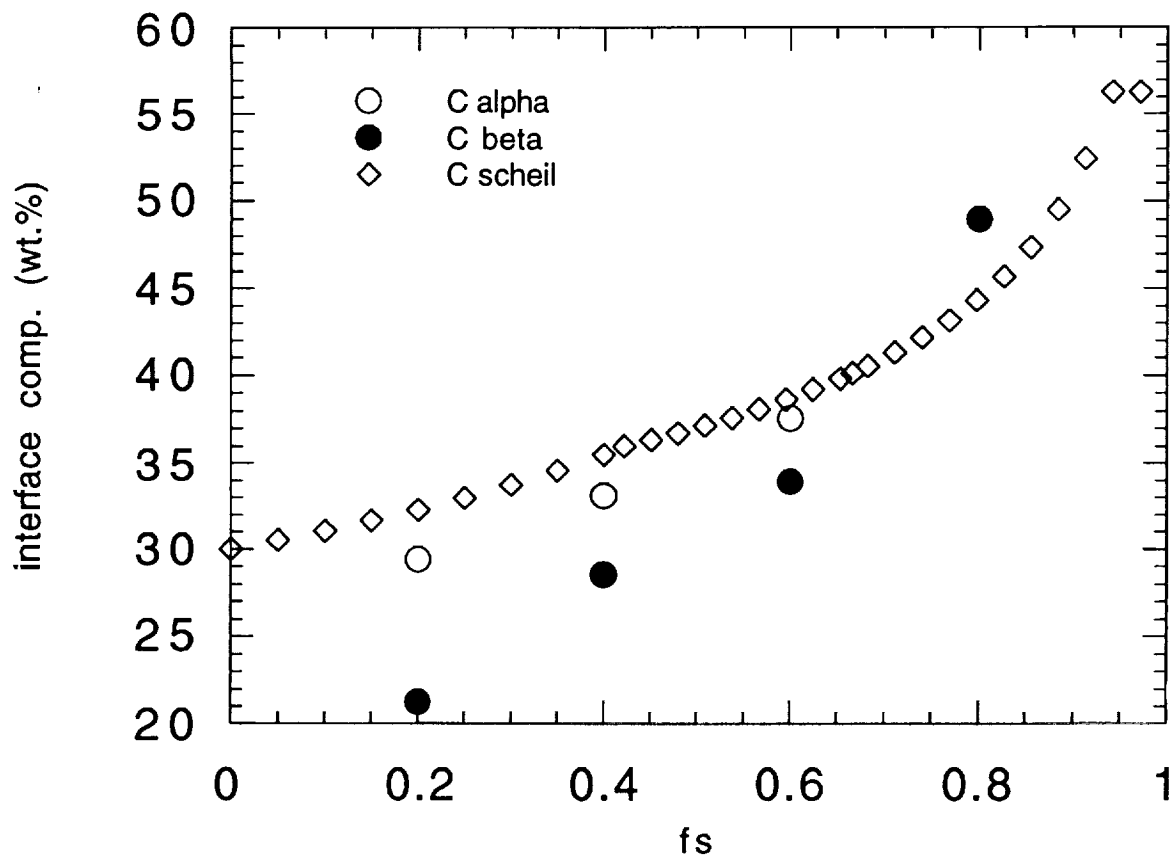
Figure 18. Interface composition as a function of fraction solid as determined from the measured temperature profiles by assumption of local equilibrium and comparison with the Scheil equation For V=.75 μm/sec.
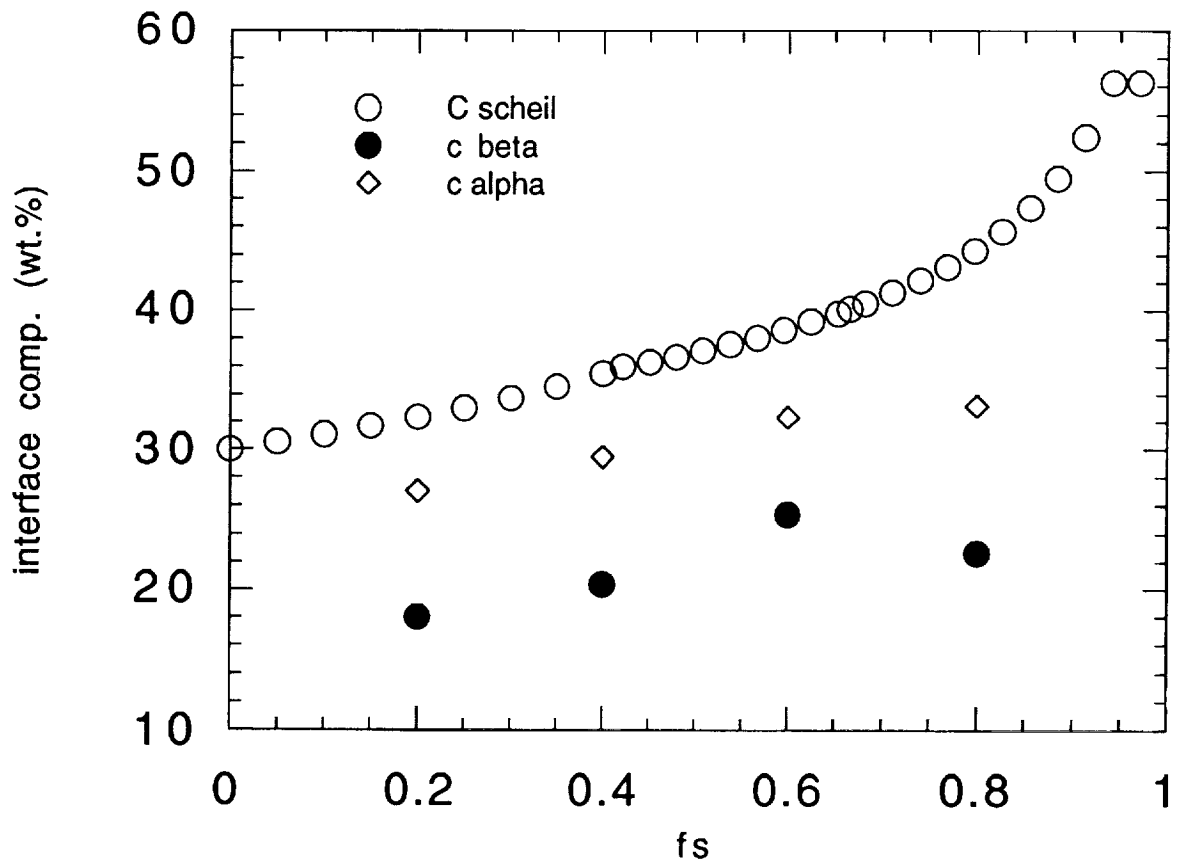
Figure 19. Interface composition as a function of fraction solid as determined from the measured temperature profiles by assumption of local equilibrium and comparison with the Scheil equation For V=.75 μm/sec.